DE GRUYTER OPEN

10.2478/mecdc-2014-0009

COMPUTATIONAL MODELLING OF PISTON RING DYNAMICS IN 3D

JOZEF DLUGOŠ, PAVEL NOVOTNÝ
Institute of Automotive Engineering, Brno University of Technology, Technická 2, CZ 616 69 Brno, Czech Republic
Tel.: +420 541 142 262, Fax: +420 541 143 354, E-mail: y125974@stud.fme.vutbr.cz

SHRNUTÍ
Pokročilé výpočtové modely pístní skupiny na základě virtuálních prototypů vyžadují mimo jiné i detailní popis dynamického chování pístního kroužku. Z tohoto hlediska je zřejmé, že pístní kroužky pracují v podmínkách, které obecně nelze zjednodušit na často využívaný osově symetrický model. Píst a vložka válce nemají dokonale kruhový tvar především v důsledku výrobních tolerancí a vnějšího tepelně-mechanického zatížení. V případech, kdy kroužek nedokáže kopírovat deformace vložky, nastane lokální ztráta kontaktu a následně i zvýšený profuk spalin a spotřeba oleje. V současné době využívané výpočtové modely nejsou schopné zahrnout všechny podstatné efekty. Článek se zaměřuje na tvorbu 3D poddajného modelu pístního kroužku s využitím Timoshenkovy teorie prutů a Multibody systému (MBS). Vytvořený výpočetní model je porovnán s numerickým řešením na základě metody konečných prvků (FEM).
KLÍČOVÁ SLOVA: PÍSTNÍ KROUŽEK, TIMOSHENKOVA TEORIE NOSNÍKU, MECHANICKÉ ZTRÁTY, MBS

ABSTRACT
Advanced computational models of a piston assembly based on the level of virtual prototypes require a detailed description of piston ring behaviour. Considering these requirements, the piston rings operate in regimes that cannot, in general, be simplified into an axisymmetric model. The piston and the cylinder liner do not have a perfect round shape, mainly due to machining tolerances and external thermo-mechanical loads. If the ring cannot follow the liner deformations, a local loss of contact occurs resulting in blow-by and increased consumption of lubricant oil in the engine. Current computational models are unable to implement such effects. The paper focuses on the development of a flexible 3D piston ring model based on the Timoshenko beam theory using the multibody system (MBS). The MBS model is compared to the finite element method (FEM) solution.
KEYWORDS: PISTON RING, TIMOSHENKO BEAM THEORY, MECHANICAL LOSSES, MULTIBODY SYSTEM

1. INTRODUCTION
A piston ring is a split ring used in internal combustion engines for three main functions:

- to seal the combustion chamber against the transfer of the gasses into the crankcase,
- to ensure heat flow from the piston to the cylinder, and
- to prevent oil not needed for lubrication from passing from the crankcase into the combustion chamber, and to provide a uniform oil film on the cylinder bore surface.

These requirements have to be met with respect to demands such as low friction, low wear, emission suppression, good resistance against thermo-mechanical fatigue, reliable operation, and cost effectiveness in order to achieve high power efficiency and a long operational life.

The largest portion of the engine's mechanical losses can be linked to the piston assembly due to the friction forces between the piston/cylinder liner and the piston ring pack/cylinder liner as demonstrated in Figure 1. The primary benefit of friction reduction is obvious – less fuel consumption and hence a reduction in CO_2 emissions.

2. TIMOSHENKO BEAM THEORY
Some features of modern engineering mechanics are based on the Stephen Timoshenko theory, which has the following limitations:

- a beam is defined by the neutral axis and cross section,
- the neutral axis is a continuous function in both the undeformed and the deformed state,

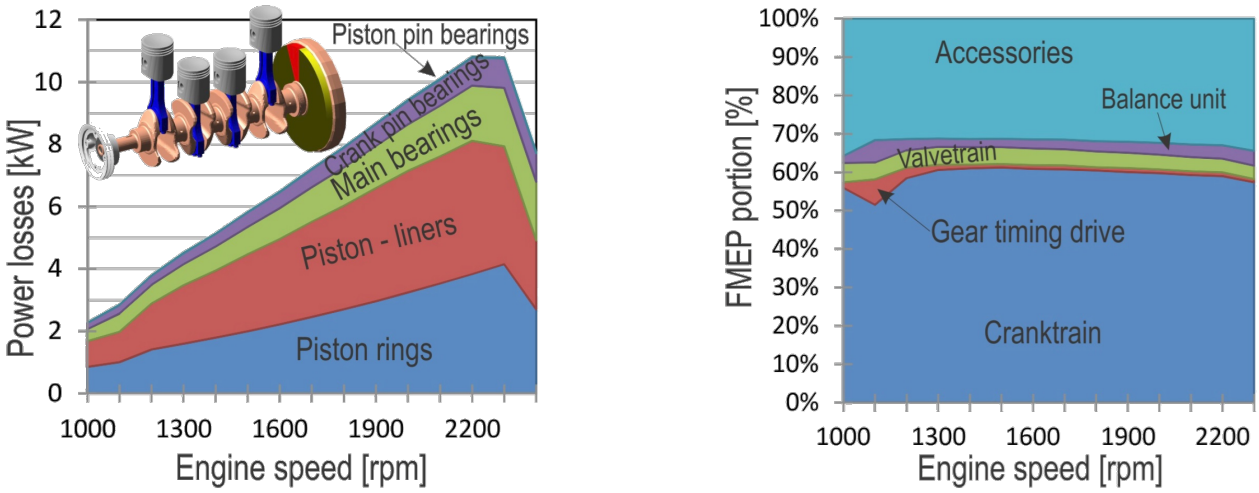

FIGURE 1: Mechanical loss contribution in a 4.2L diesel engine [1]
OBRÁZEK 1: Podíl mechanických ztrát 4.2L naftového motoru [1]

- the cross section is planar before and after loading – no warping or out-of-plane distortion occurs. Warping greatly complicates the behaviour of the beam,
- all loads act through the centroid of the cross-sectional area,
- an assumption of small deflections,
- the beam is perfectly elastic – it recovers its original shape completely after unloading.

Figure 2 presents a beam model, where a, b and c are angles of rotation while u, v and w are deflections.

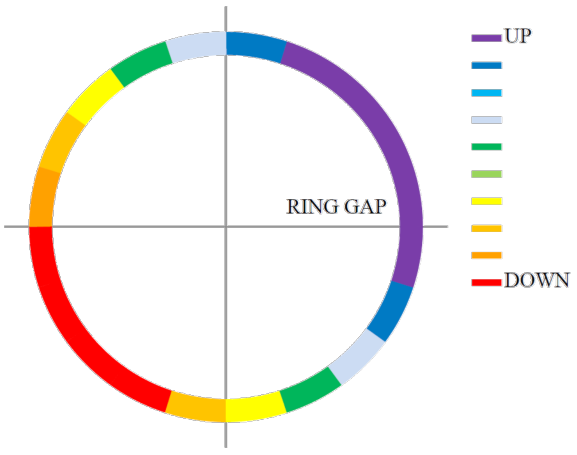

FIGURE 2: Beam model
OBRÁZEK 2: Model prutu

The Timoshenko beam theory does not neglect shear deformation effects for bending of beams, i.e. sections that are originally perpendicular to the neutral axis may not be perpendicular to the neutral axis after the deformation. This effect is most significant in the case of stocky beams. The relationship between the load and the deformation, according to the Timoshenko beam theory, is defined as

$$\begin{bmatrix} F_x \\ F_y \\ F_z \\ M_x \\ M_y \\ M_z \end{bmatrix} = \begin{bmatrix} \frac{AE}{l} & 0 & 0 & 0 & 0 & 0 \\ & \frac{12EI_z}{l^3(1+P_y)} & 0 & 0 & 0 & \frac{-6EI_z}{l^2(1+P_y)} \\ & & \frac{12EI_y}{l^3(1+P_z)} & 0 & \frac{6EI_y}{l^2(1+P_z)} & 0 \\ & & & \frac{I_pG}{l} & 0 & 0 \\ & & & & \frac{(4+P_z)EI_y}{l(1+P_z)} & 0 \\ & & sym. & & & \frac{(4+P_y)EI_z}{l(1+P_y)} \end{bmatrix} \begin{bmatrix} u \\ v \\ w \\ a \\ b \\ c \end{bmatrix} \tag{1}$$

where *the square matrix* represents the universal beam stiffness matrix. In this matrix I_p is the polar moment of inertia. Parameter P_y is defined to give relative importance of the shear deformations to the bending deformations in the y direction as

$$P_y = \frac{12EI_z f_{s,y}}{GAl^2}, \tag{2}$$

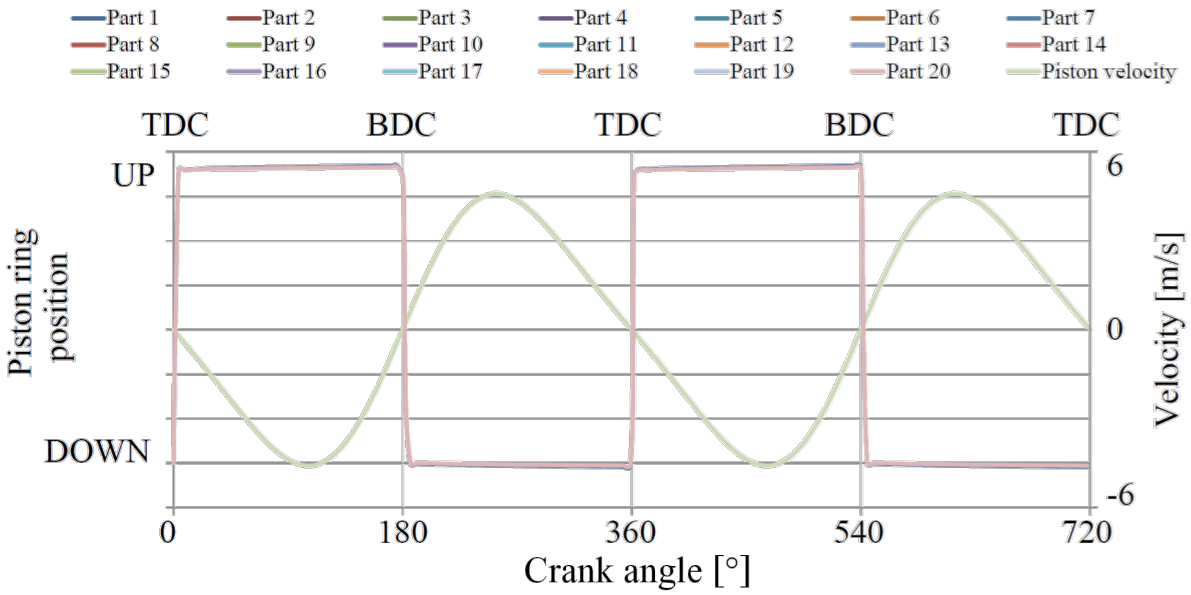

FIGURE 3: Discretized piston ring model
OBRÁZEK 3: Diskretizovaný model pístního kroužku

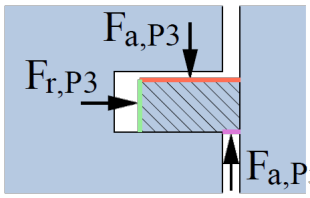

FIGURE 4: Piston ring first mode shape at eigen frequency 126 Hz estimated by FEA
OBRÁZEK 4: První vlastní tvar kmitu pístního kroužku při vlastní frekvenci 126 Hz určený pomocí MKP

where E is the modulus of elasticity, I_z (I_y) is the cross section moment of inertia in the z (y) direction, $f_{s,y}$ is the form factor for shear in the y direction, G is the shear modulus, A is the cross-sectional area and l is the length of the beam. Form factor values for typical cross sections may be found in [2]. Parameter P_z is defined analogically. It is evident that with the increasing beam length the parameters P_y and P_z reach zero, so the effect of the shear deflection due to shear force can be neglected. A more detailed derivation is available in [3].

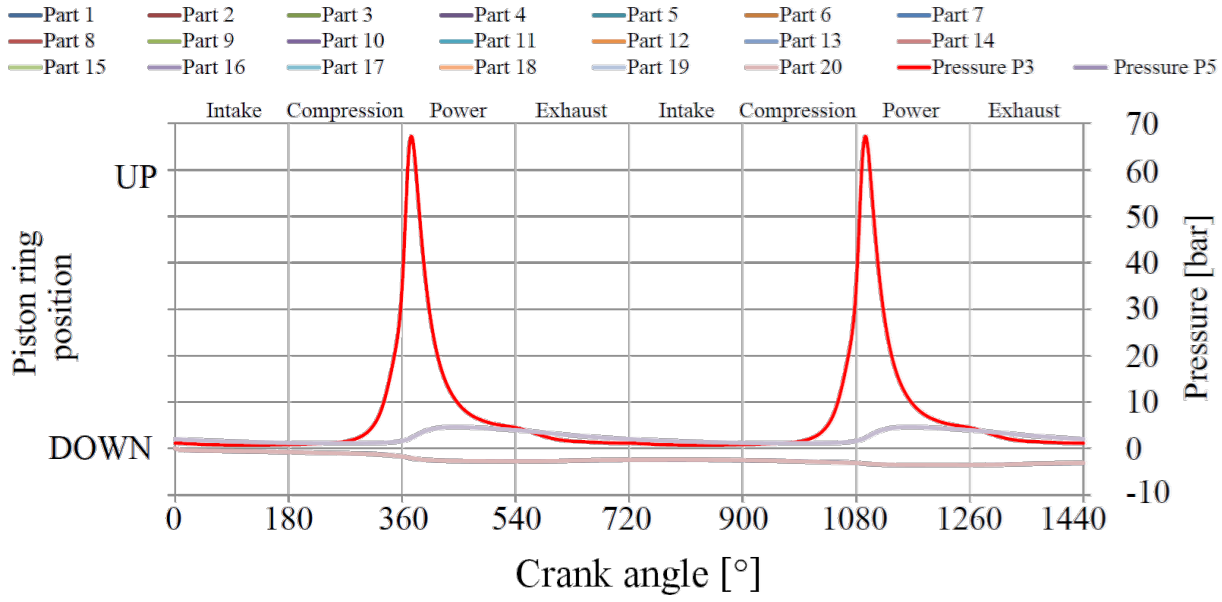

FIGURE 5: ADAMS and ANSYS natural frequency comparison
OBRÁZEK 5: Porovnání vlastních frekvencí s využitím software ADAMS a ANSYS

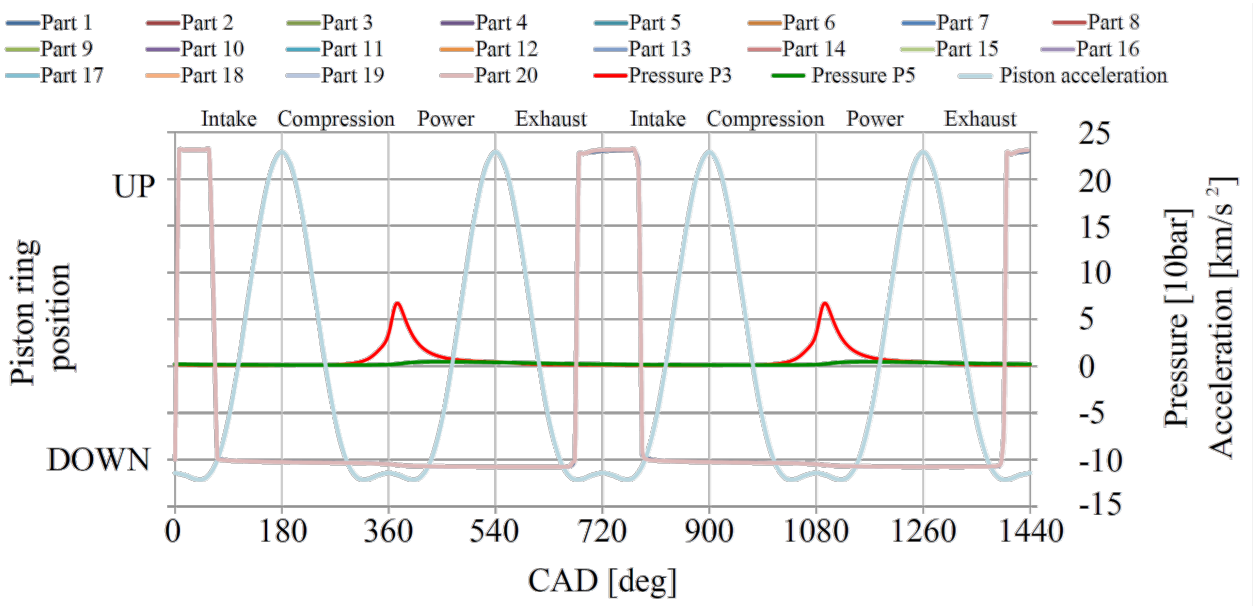

FIGURE 6: Contact pressure distribution on the ring face
OBRÁZEK 6: Rozložení kontaktního tlaku na čele pístního kroužku

3. PISTON RING DISCRETIZATION AND VALIDATION

The piston ring is divided using the MBS software MSC Adams into n rigid segments connected to its neighbours by a stiffness matrix defined by the square matrix presented in (1).

Figure 3 illustrates the piston ring discretization (gaps between segments are only for better demonstration and do not appear in the real model).

Undamped natural frequency depends on the stiffness and the mass properties of the object. Discretizing the piston ring did not change its mass (no material removal). Therefore, the natural frequency can be used as a parameter suitable for comparing the two different stiffness estimation methods while the mass characteristics remain the same. The piston ring is also modelled in FEM using ANSYS software, and natural frequencies and mode shapes are calculated. Figure 4 depicts the total displacement of the piston ring first mode shape.

Results presented in Figure 5 reflect a very good correlation between the discretization in MBS and FEM software – all natural frequencies below 1100 Hz estimated by MBS have limit values equal to the frequencies obtained from FEM. Segment count $n = 20$ is set as the best compromise between the accuracy and the computing time, since the differences between MBS and FEM results of all 6 natural frequencies are below 5 %.

3.1 CONTACT ANALYSIS

Contact analysis between the piston ring and the cylinder liner is conducted in order to discover differences between the contact

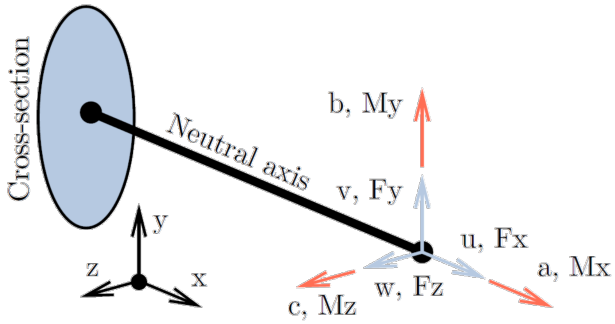

FIGURE 7: Piston assembly model
OBRÁZEK 7: Model sestavy pístní skupiny

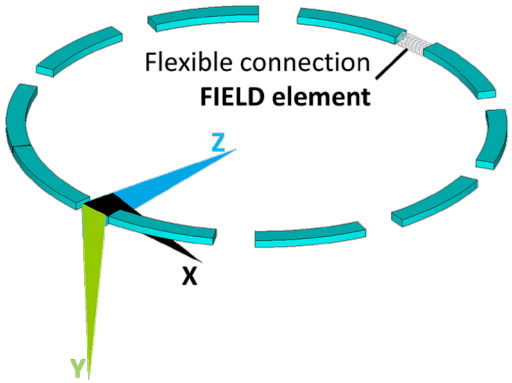

FIGURE 8: Piston ring motion for engine speed of 1000 rpm with inertia only
OBRÁZEK 8: Pohyb pístního kroužku pouze se setrvačností pro otáčky motoru 1000 min^{-1}

pressure distribution estimated by the FEM and by the MBS software. The results are augmented by an analytical solution

$$p = \frac{2F_t}{dh}\,, \tag{3}$$

where p is the contact pressure, F_t is the pretension force, d is the piston ring nominal diameter and h is the piston ring width. Distribution of the contact pressure along the circumference of the piston ring face (Figure 6) is very similar i.e. the piston ring discretization in MBS (20 rigid segments) is adequate and does represent a much larger FEM model adequately. The ring gap region (0 deg and 360 deg) is the area most affected by the pretension force applied and hence results in the biggest difference in comparison with the analytical solution.

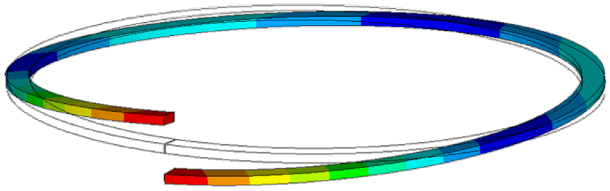

FIGURE 9: Piston ring motion for engine speed of 40 rpm with inertia only
OBRÁZEK 9: Pohyb pístního kroužku pouze se setrvačností pro otáčky motoru 40 min^{-1}

4. PISTON RING/CYLINDER LINER MODEL

Figure 7 presents the model used for investigation of piston ring behaviour. The cylinder liner is drawn only as a plane for better demonstration, but its actual shape is a hollowed cylinder. The piston is constrained to move only vertically and the motion is

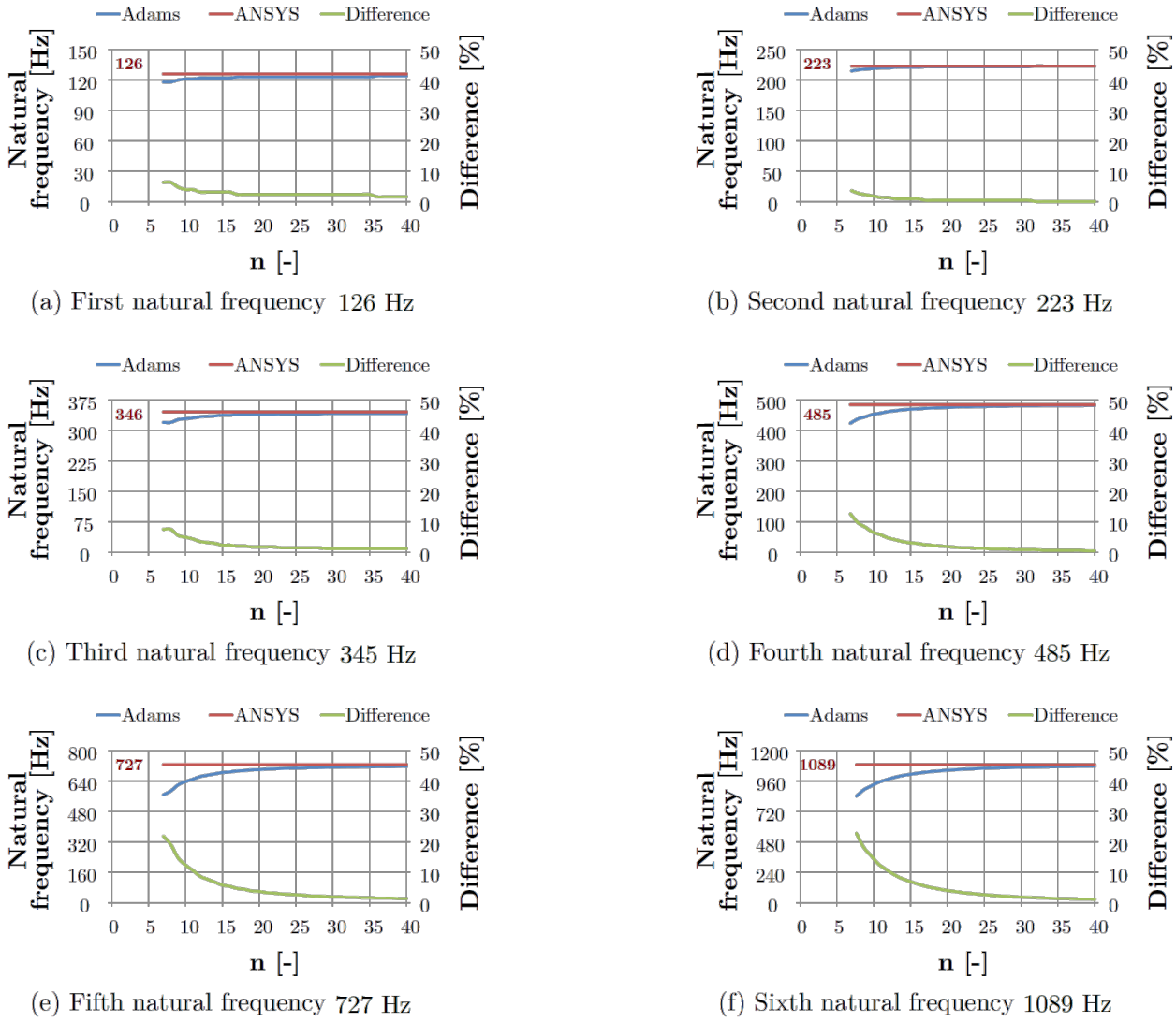

(a) First natural frequency 126 Hz
(b) Second natural frequency 223 Hz
(c) Third natural frequency 345 Hz
(d) Fourth natural frequency 485 Hz
(e) Fifth natural frequency 727 Hz
(f) Sixth natural frequency 1089 Hz

FIGURE 10: Stuck piston ring for crank angle position 180° and engine speed of 40 rpm
OBRÁZEK 10: Zastavený pístní kroužek pro rozsah natočení kliky 180° a otáčky motoru 40 min^{-1}

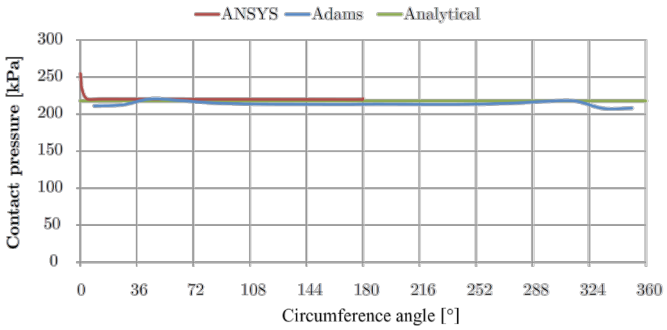

FIGURE 11: Piston ring motion for engine speed of 1000 rpm with friction applied
OBRÁZEK 11: Pohyb pístního kroužku se zadaným třením pro otáčky motoru 1000 min^{-1}

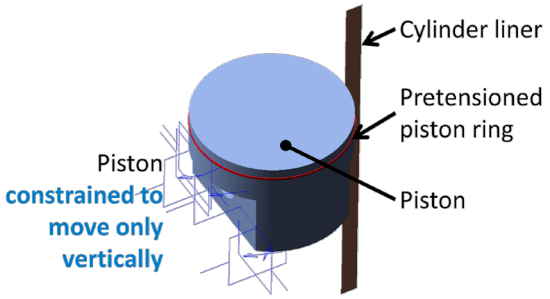

FIGURE 12: Applied gas pressure forces
OBRÁZEK 12: Uvažované síly od tlaku spalin

applied as a displacement function of the crank mechanism in the piston pin. The pretension force of the piston ring is applied on the ring end faces.

4.1 INERTIA ONLY

In this case, no influences (no friction or gas pressure) other than the pretension and the inertia forces are considered. Therefore, the piston ring should reflect the acceleration – the predicted piston ring motion is a slap motion from the bottom to the top position in the piston groove. This prediction is fulfilled in the case of higher rotary speeds. Calculation of the piston ring movement at a rotary speed of 1000 rpm is depicted in Figure 8. On the other hand, for the low rotary speeds (e.g. 40 rpm as presented in Figure 9) the inertia forces are very low and are not able to overcome the influence of the pretension, which causes the ring to become stuck in the groove (Figure 10), where it remains, only minimally affected by the inertia forces.

4.2 FRICTION ONLY

The friction is specified by the coefficient of friction as a constant value of 0.1 [4]. The piston ring motion should reflect the piston velocity (unlike the previous model), and this is confirmed by the simulation results in Figure 11.

4.3 FRICTION AND GAS PRESSURE APPLIED

Three gas pressure forces are applied on the piston ring surfaces as depicted in Figure 12. The force values are equal to the pressure acting on the constant surface – and that is the stumbling block of this approach. The piston ring area, affected by the gas pressure, varies throughout the engine operation cycle and is not constant at all.

As presented by Isarai et al. [5], during the intake stroke the piston ring should be sucked to the top side of the piston groove.

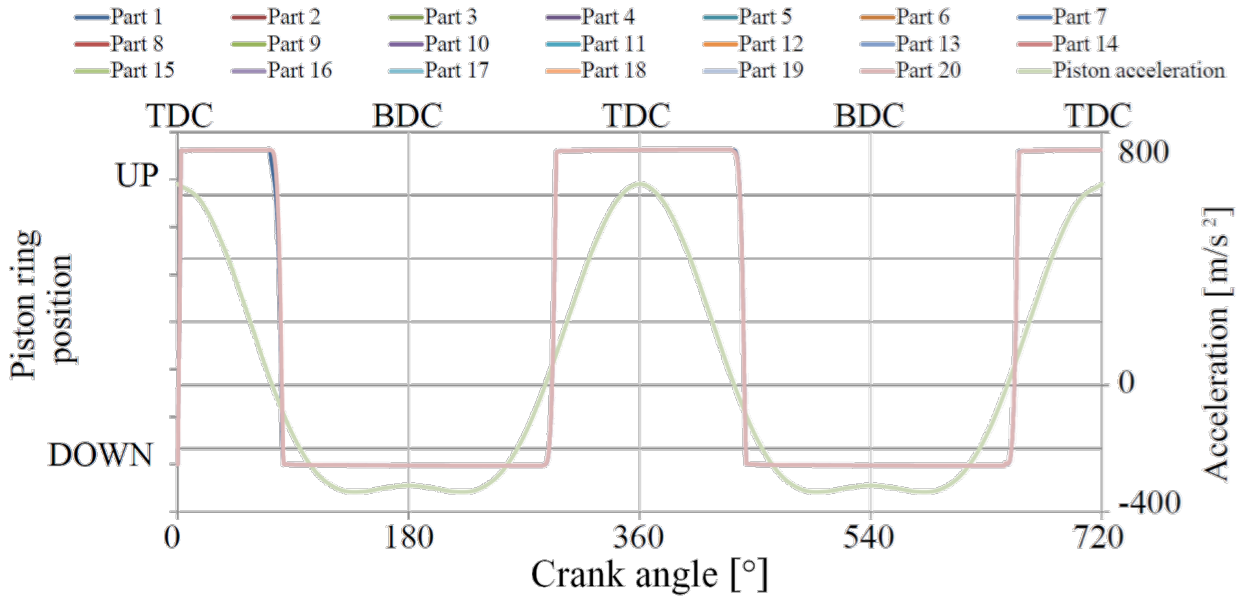

FIGURE 13: Piston ring motion for engine speed of 1000 rpm with friction forces and gas pressures applied
OBRÁZEK 13: Pohyb pístního kroužku se zadanými silami třecími a od tlaku spalin pro otáčku motoru 1000 min^{-1}

In this case, results in Figure 13 show that the piston ring is unable to move vertically.

At a higher rotary speed of 6000 rpm, the inertia and friction forces after a certain threshold overcome the axial gas pressure force and the piston ring moves upwards (Figure 14). This happens only at the end of the exhaust and the beginning of the intake stroke – the portion of the cycle where the acceleration is high and conversely, the gas pressure is low.

To ensure the proper behaviour an iterative gas pressure force evaluation, depending on the active area, is mandatory.

5. CONCLUSION

The piston ring is discretized by rigid segments connected via flexible elements which use the Timoshenko beam theory for the stiffness matrix estimation. The idea is to keep the piston ring model within a single software package to minimize possible user errors and the number of licenses needed. In addition, the developed method is automated and quick. The inputs are the piston ring geometry, material, pretension force and segment count.

The validated 3D flexible piston ring model serves as a basis for further very complex piston ring dynamics modelling – on each piston ring rigid segment nodes (markers, local coordinate systems) are generated and then the equilibrium equations are formed and solved. Such approach leads to a model able to work with distorted bore shapes with full piston ring geometry including the ring gap, with general piston ring deflections and motion, or able to include the twist effects of unsymmetrical ring cross sections (L-shaped, tapered etc.).

REFERENCES

[1] Novotný P., Píštěk V., Svída D. (2010). Solution of powertrain friction losses by virtual engine, In: MECCA – Journal of Middle European Construction and Design of Cars, pp. 12–61. ISSN 1214-0821

[2] Timoshenko S. P., Gere J. M. (1991). Mechanics of Materials, Third IS edition, London: Chapman & Hall. ISBN 0-412-36880-3

[3] Dlugoš J. (2014). Computational Modelling of Piston Ring Dynamics, Master's thesis, Brno University of Technology

[4] Andersson, P., Tamminen, J., Sandström, C. (2002). Piston ring tribology, VTT Research Notes 2178, VTT. ISBN 951-38-6107-4

[5] Isarai R., Sugino M., Moritsugu M., Kato N., Nakamura M. (2008). Strain and Motion Measurement for Piston, Piston Ring and Connecting Rod of High Speed Running Engines using New Digital Telemeter, Society of Automotive Engineers, Inc., SAE Technical Paper 2008-01-1042. ISSN 0148-7191

ACKNOWLEDGEMENT

This work is an output of NETME CENTRE PLUS research activities (project no. LO1202) and is funded by the Ministry of Education, Youth and Sports under the *National Sustainability Programme I.*

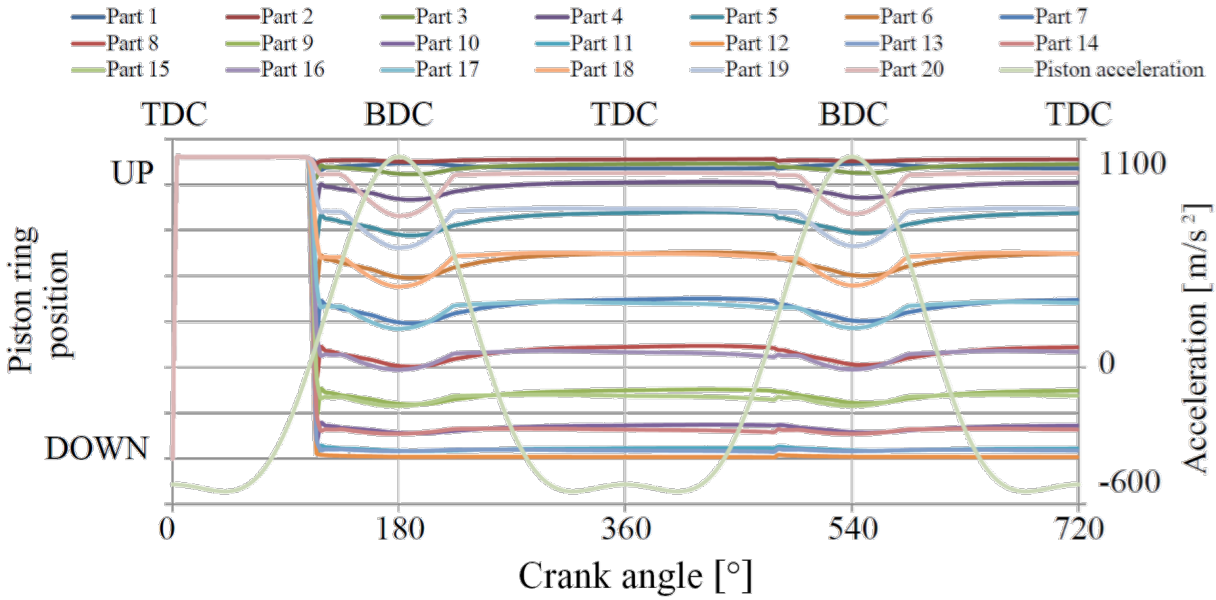

FIGURE 14: Piston ring motion for engine speed of 6000 rpm with friction forces and gas pressures applied
OBRÁZEK 14: Pohyb pístního kroužku se zadanými silami třecími a od tlaku spalin pro otáčku motoru 6000 min^{-1}